Stokes–Mueller matrix polarimetry technique for circular dichroism/birefringence sensing with scattering effects

Quoc-Hung Phan
Yu-Lung Lo

Stokes–Mueller matrix polarimetry technique for circular dichroism/birefringence sensing with scattering effects

Quoc-Hung Phan[a] and Yu-Lung Lo[a,b,*]
[a]National Cheng Kung University, Mechanical Engineering Department, Tainan, Taiwan
[b]National Cheng Kung University, Advanced Optoelectronic Technology Center, Tainan, Taiwan

Abstract. A surface plasmon resonance (SPR)-enhanced method is proposed for measuring the circular dichroism (CD), circular birefringence (CB), and degree of polarization (DOP) of turbid media using a Stokes–Mueller matrix polarimetry technique. The validity of the analytical model is confirmed by means of numerical simulations. The simulation results show that the proposed detection method enables the CD and CB properties to be measured with a resolution of 10^{-4} refractive index unit (RIU) and 10^{-5} RIU, respectively, for refractive indices in the range of 1.3 to 1.4. The practical feasibility of the proposed method is demonstrated by detecting the CB/CD/DOP properties of glucose–chlorophyllin compound samples containing polystyrene microspheres. It is shown that the extracted CB value decreases linearly with the glucose concentration, while the extracted CD value increases linearly with the chlorophyllin concentration. However, the DOP is insensitive to both the glucose concentration and the chlorophyllin concentration. Consequently, the potential of the proposed SPR-enhanced Stokes–Mueller matrix polarimetry method for high-resolution CB/CD/DOP detection is confirmed. Notably, in contrast to conventional SPR techniques designed to detect relative refractive index changes, the SPR technique proposed in the present study allows absolute measurements of the optical properties (CB/CD/DOP) to be obtained. © *2017 Society of Photo-Optical Instrumentation Engineers (SPIE)* [DOI: 10.1117/1.JBO.22.4.047002]

Keywords: Stokes–Mueller matrix polarimetry; surface plasmon resonance; circular dichroism; circular birefringence.

Paper 160789R received Nov. 16, 2016; accepted for publication Mar. 22, 2017; published online Apr. 6, 2017.

1 Introduction

Polarization is a fundamental property of light and has many practical applications in industry and engineering science. Many studies have shown that the polarization state of a light beam (including depolarization effects) can be fully described by four Stokes parameters (S_0, S_1, S_2, and S_3).[1–3] Meanwhile, the change in optical properties of a sample given different polarization states of the incident light can be completely described by the Mueller matrix formalism.[4] Consequently, Stokes–Mueller matrix polarimetry provides a powerful technique for characterizing a wide range of materials, biomaterials, and turbid media.[5,6] Lu and Chipman[7] proposed a pioneering method for dealing with the strong multiple scattering effects of turbid media by decomposing the Mueller matrix into a sequence of three matrix factors corresponding to the diattenuation, retardation, and depolarization properties, respectively. Kumar et al.[8] and Ghosh and Vitkin[9] utilized polar decomposition and Mueller matrix decomposition methods to extract/quantify the linear retardance, optical rotation, and depolarization parameters of complex tissue-like turbid media with simultaneous scattering and depolarization effects. Pham and Lo[10,11] proposed a Stokes–Mueller decomposition matrix-based method for extracting all the effective parameters of turbid media, including the linear birefringence, linear dichroism, circular birefringence (CB), circular dichroism (CD), linear depolarization, and circular depolarization properties. However, the methods in Refs. 8–11 require a strict decoupling of the

optical properties of the sample. As a result, they are unsuitable for samples containing multiple properties. Several studies have shown that this problem can be resolved by a differential Mueller matrix formalism. Quijano et al.[12] proposed a differential Mueller matrix decomposition method for extracting the polarimetric properties of general depolarizing anisotropic media. Liao and Lo[13] developed a hybrid model comprising the Mueller matrix decomposition method and the differential Mueller matrix formalism for obtaining full-range measurements of the anisotropic optical properties of turbid media. However, the methods in Refs. 12 and 13 require light to be transmitted through the sample and are thus unsuitable for noninvasive practical medical diagnoses.

Surface plasmon resonance (SPR) is a charge density oscillation at the interface of two media with dielectric constants of opposite signs and has significant potential for sensing applications.[14–16] Generally speaking, existing SPR sensors are based on either prism couplers or diffraction gratings. Of the two types of sensor, those based on prism couplers tend to have a better sensitivity and resolution.[17] One of the most common uses of prism coupler-based SPR sensors is that of total internal reflection ellipsometry (TIRE).[18] Le et al.[19] used TIRE to visualize the behavior of giant lipid vesicles interacting with an adhesive surface coated with poly-L-lysine. Olender et al.[20] used TIRE to perform the real-time monitoring of the absorption of lipopolysaccharide molecules and whole gram-negative bacteria cells. Balevicius et al.[21,22] utilized TIRE to study the

interaction of biomolecule layers and the optical anisotropy of biorecognition molecule layers.

In a previous study,[23] the present group proposed an SPR-based technique for enhanced CD/degree of polarization (DOP) sensing. In the present study, the proposed method is extended to the detection of the CB/CD/DOP properties of complex turbid media. The validity of the proposed method is demonstrated both numerically and by means of experimental investigations using glucose–chlorophyllin compound samples containing polystyrene microspheres.

2 Total Internal Reflection Ellipsometry Surface Plasmon Resonance Prism Coupler

Figure 1(a) presents a schematic illustration of the SPR prism coupler used in the present study. As described in Ref. 23, the coupler comprises a half-ball glass lens, a Cr–Au isotropic thin-film layer, and a Ta_2O_5 anisotropic layer. The half-ball lens couples the incident polarized light into the isotropic and anisotropic films and provides total internal reflection. Meanwhile, the isotropic and anisotropic layers enhance the sensing performance by manipulating the incident polarized light and inducing SPR at the sensed interface. The half-ball lens in the SPR prism coupler was fabricated of BK7 glass with a refractive index of $n_0 = 1.517$. The refractive indices of the isotropic and anisotropic layers were the same as those in Ref. 23, i.e., $n_1 = 0.36\text{–}2.9i$, $n_{21} = 1.637$; and $n_{22} = 1.449$, $n_{23} = 1.589$. However, the thicknesses of the two layers were increased to $d_1 = 30$ nm and $d_2 = 10$ nm, respectively, to improve the measurement sensitivity of the CB/CD/DOP properties. The resonance angle of the prism coupler was found to be around 76 deg at a wavelength of 632.8 nm and resulted in a reflectance coefficient R_{pp} of <0.2, as shown in Fig. 1(b).

3 Analytical Model for Extracting Circular Birefringence/Circular Dichroism/Degree of Polarization Properties

An optical sample can be described by the matrix formulation $S = MS'$, where S is the Stokes vector of the output light, M is the 4×4 Mueller matrix of the sample, and S' is the Stokes vector of the input light. The general form of this relation is given as follows:

$$\begin{bmatrix} S_1 \\ S_2 \\ S_3 \\ S_4 \end{bmatrix} = \begin{bmatrix} M_{11} & M_{12} & M_{13} & M_{14} \\ M_{21} & M_{22} & M_{23} & M_{24} \\ M_{31} & M_{32} & M_{33} & M_{34} \\ M_{41} & M_{42} & M_{43} & M_{44} \end{bmatrix} \begin{bmatrix} S'_0 \\ S'_1 \\ S'_2 \\ S'_3 \end{bmatrix}. \tag{1}$$

Compared to the model presented in Ref. 23 for CD/DOP measurement, the Mueller matrix in the present study contains an additional term (M_{CB}) to describe the CB properties of the sample. In other words, the Mueller matrix is given by

$$M_{sample} = M_{CB} M_{CD} M_R M_D, \tag{2}$$

where M_{CD}, M_R, and M_D are the Mueller matrices of the CD property, the reflectance of the prism coupler, and the scattering-induced depolarization effect, respectively.[23] For a CB sample with a circular optical rotation angle γ, M_{CB} has the form:[10]

$$M_{CB} = \begin{bmatrix} 1 & 0 & 0 & 0 \\ 0 & \cos(2\gamma) & \sin(2\gamma) & 0 \\ 0 & -\sin(2\gamma) & \cos(2\gamma) & 0 \\ 0 & 0 & 0 & 1 \end{bmatrix}. \tag{3}$$

Thus, Eq. (1) can be expressed as follows:

$$\begin{bmatrix} S_0 \\ S_1 \\ S_2 \\ S_3 \end{bmatrix} = \begin{bmatrix} M_{11} & M_{12} & M_{13} & M_{14} \\ M_{21} & M_{22} & M_{23} & M_{24} \\ M_{31} & M_{32} & M_{33} & M_{34} \\ M_{41} & M_{42} & M_{34} & M_{44} \end{bmatrix} \begin{bmatrix} S'_0 \\ S'_1 \\ S'_2 \\ S'_3 \end{bmatrix} = M_{CB} M_{CD} M_D M_R \begin{bmatrix} S'_0 \\ S'_1 \\ S'_2 \\ S'_3 \end{bmatrix}$$

$$= \begin{bmatrix} m_{11}(R^2+1)+m_{12}p_1(R^2+1) & m_{12}(R^2+1)+m_{11}p_1(R^2+1) & M_{13} & M_{14} \\ -e_1 m_{12}\cos(2\gamma)(R^2-1) & -e_1 m_{11}\cos(2\gamma)(R^2-1) & -e_2 m_{33}\sin(2\gamma)(R^2-1) & -e_2 m_{34}\sin(2\gamma)(R^2-1) \\ e_1 m_{12}\sin(2\gamma)(R^2-1) & e_1 m_{11}\sin(2\gamma)(R^2-1) & -e_2 m_{33}\cos(2\gamma)(R^2-1) & -e_2 m_{34}\cos(2\gamma)(R^2-1) \\ 2Rm_{11}+2Rp_1 m_{12} & 2Rm_{12}+2Rp_1 m_{11} & M_{34} & M_{44} \end{bmatrix} \begin{bmatrix} S'_0 \\ S'_1 \\ S'_2 \\ S'_3 \end{bmatrix}, \tag{4}$$
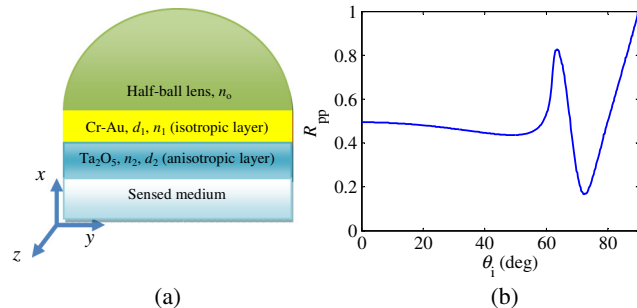
where

$$M_{13} = m_{33}p_2(R^2+1) - m_{34}[2Re_3 + p_3(R^2+1)], \tag{5}$$

$$M_{14} = m_{34}p_2(R^2+1) + m_{33}[2Re_3 + p_3(R^2+1)], \tag{6}$$

$$M_{34} = 2Rm_{33}p_2 - m_{34}[2Rp_3 + e_3(R^2+1)], \tag{7}$$

$$M_{44} = 2Rm_{34}p_2 + m_{33}[2Rp_3 + e_3(R^2+1)]. \tag{8}$$

Fig. 1 (a) Schematic illustration of SPR prism coupler and (b) resonance angle determination.

Note that R is the CD property of the sample; m_{11}, m_{12}, m_{33} and m_{34} are the elements of the M_R Mueller matrix; and p_1, p_2, p_3, e_1, e_2, and e_3 are the elements of the M_D Mueller matrix.

As described in the following, the use of four input lights [namely, three linear polarization lights (0, 45, and 90 deg) and one right-hand circular polarization light] yields a sufficient number of equations to determine parameters γ, R, and Δ (DOP) of the optical sample. The Stokes vectors of the four input lights are given as follows: $S'_{0\ \mathrm{deg}} = [1,1,0,0]^T$, $S'_{45\ \mathrm{deg}} = [1,0,1,0]^T$, $S'_{90\ \mathrm{deg}} = [1,-1,0,0]^T$, and $S'_R = [1,0,0,1]^T$. Thus, R and γ can be obtained directly as follows:

$$R = \begin{cases} \dfrac{S_{0\ \mathrm{deg}}(3)}{S_{0\ \mathrm{deg}}(0)} + \sqrt{\left[\dfrac{S_{0\ \mathrm{deg}}(3)}{S_{0\ \mathrm{deg}}(0)}\right]^2 - 1}, & -1 \le R < 0, R \ne 0 \\[4mm] \dfrac{S_{0\ \mathrm{deg}}(3)}{S_{0\ \mathrm{deg}}(0)} - \sqrt{\left[\dfrac{S_{0\ \mathrm{deg}}(3)}{S_{0\ \mathrm{deg}}(0)}\right]^2 - 1}, & 0 < R \le -1, R \ne 0 \end{cases}, \quad (9)$$

$$\gamma = \begin{cases} -\arctan\dfrac{S_{0\ \mathrm{deg}}(2)}{S_{0\ \mathrm{deg}}(1)}, & 0\ \mathrm{deg} < \gamma \le 45\ \mathrm{deg} \\[3mm] -\arctan\dfrac{S_{0\ \mathrm{deg}}(2)}{S_{0\ \mathrm{deg}}(1)} + \dfrac{\pi}{2}, & 45\ \mathrm{deg} < \gamma \le 135\ \mathrm{deg} \\[3mm] -\arctan\dfrac{S_{0\ \mathrm{deg}}(2)}{S_{0\ \mathrm{deg}}(1)} + \pi, & 135\ \mathrm{deg} < \gamma < 180\ \mathrm{deg} \end{cases}. \quad (10)$$

In addition, the elements of the depolarization Mueller matrix are obtained as follows:

$$e_1 = \frac{1}{(R^2+1)} \times \frac{-[S_{0\ \mathrm{deg}}(1) + S_{90\ \mathrm{deg}}(1)]}{2m_{12}} \times \frac{1}{\cos(2\gamma)}, \quad (11)$$

$$e_2 = \frac{1}{(R^2-1)} \times \frac{2S_{45\ \mathrm{deg}}(2) - [S_{0\ \mathrm{deg}}(2) + S_{90\ \mathrm{deg}}(2)]}{2m_{33}} \times \frac{1}{\cos(2\gamma)}, \quad (12)$$

$$e_3 = \frac{4R^2 - (R^2+1)^2}{2RY - X(R^2+1)}, \quad (13)$$

$$p_1 = \frac{1}{2R} \times \frac{[S_{0\ \mathrm{deg}}(3) + S_{90\ \mathrm{deg}}(3)]}{m_{12}} - \frac{m_{11}}{m_{12}}, \quad (14)$$

$$p_2 = \frac{1}{2R}\left(\frac{M_{43} + Xm_{34}}{m_{33}}\right), \quad (15)$$

$$p_3 = \frac{X - e_3(R^2+1)}{2R}, \quad (16)$$

where

$$X = \frac{\{2S_R(3) - [S_{0\ \mathrm{deg}}(3) + S_{90\ \mathrm{deg}}(3)]\}m_{33} - m_{34}\{2S_{45\ \mathrm{deg}}(3) - [S_{0\ \mathrm{deg}}(3) + S_{90\ \mathrm{deg}}(3)]\}}{m_{33}^2 + m_{34}^2}, \quad (17)$$

$$Y = \frac{m_{33}\{2S_R(0) - [S_{0\ \mathrm{deg}}(0) + S_{90\ \mathrm{deg}}(0)]\} - m_{34}\{2S_{45\ \mathrm{deg}}(0) - [S_{0\ \mathrm{deg}}(0) + S_{90\ \mathrm{deg}}(0)]\}}{m_{33}^2 + m_{34}^2}. \quad (18)$$

Thus, the Δ can then be obtained as follows:

$$\Delta = 1 - \sqrt{\frac{e_1^2 + e_2^2 + e_3^2}{3}}, \qquad 0 \le \Delta \le 1. \quad (19)$$

It is noted that e_1 and e_2 in Eqs. (11) and (12) are functions of γ and represent the only difference from the expressions given in Ref. 23 for the depolarization Mueller matrix.

4 Validity of Analytical Model

The validity of the analytical model derived above was investigated by comparing the values obtained for parameters Δ, γ, and R of a hypothetical sample with the known values inserted into the sample matrix in Eq. (2). In performing the simulations, the refractive index of the CB/CD/DOP sample was set as 1.33 and the incident angle θ_i was set equal to the SPR angle of 76 deg. As shown in Fig. 2, a good agreement was obtained between the two sets of values in every case. In other words,
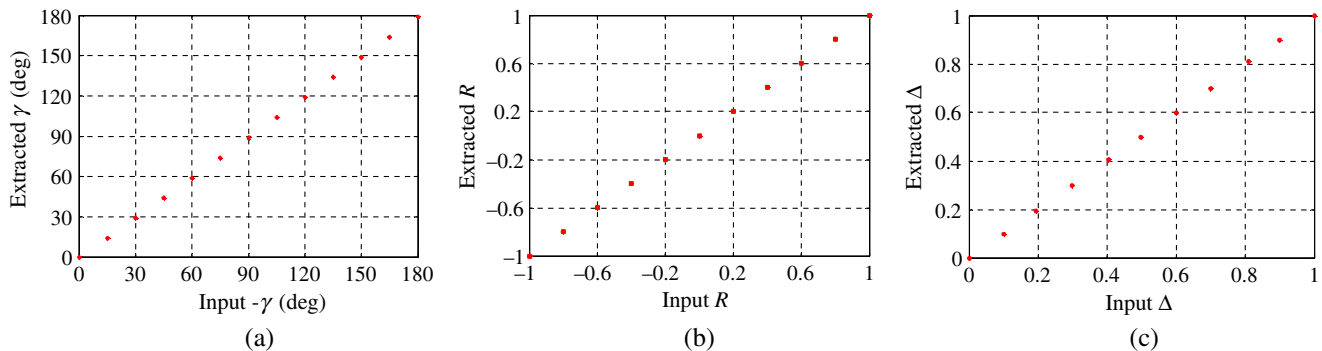

Fig. 2 Comparison of extracted values and input values of: (a) γ, (b) R, and (c) Δ.

the ability of the proposed model to extract the values of Δ, R, and γ over the full range is confirmed.

5 Sensitivity of Circular Dichroism Measurements to Chlorophyllin Concentration

Chlorophyllin is a common photosynthetic pigment and can be obtained from spinach leaves or grass. The molecular structure of chlorophyllin results in a high optical absorbance and a strong CD effect.[24,25] In the present study, simulations were performed to investigate the sensitivity of the extracted R value to the change in concentration of chlorophyllin sodium copper salt samples (referred to hereafter simply as chlorophyllin samples) in aqueous solution. In performing the simulations, the change in concentration of the chlorophyllin sample was modeled by a change in the refractive index N.[26] Based on this assumption, the R values of samples with refractive indices ranging from 1.3 to 1.4 (with a step size of 0.01) were computed using Eq. (9) for scanning angles θ in the range of 0 to 180 deg. The corresponding results are presented in Fig. 3. It is noted that scanning angle θ is the angle between the original $X - Y$ coordinate system and the measured $P' - S'$ coordinate system of the polarization scanning ellipsometry technique developed by the current group in Ref. 27. As described in Ref. 27, in applying Eq. (9) to derive the R parameter, the traditional algorithm must be modified from the laboratory ($X - Y$) coordinate system to the measured $P' - S'$ coordinate system. Thus, the axes of the four polarization input light beams (i.e., 0 deg, 45 deg, 90 deg, and $R-$) in the $P' - S'$ coordinate system must be rotated through an additional scanning angle of θ to convert them to the $X - Y$ coordinate frame.

As shown in Fig. 3(a), the extracted R values are particularly sensitive to changes in the refractive index (i.e., the chlorophyllin concentration) at scanning angles of 45 and 135 deg. Furthermore, Fig. 3(b) shows that the R value increases approximately linearly over the refractive index range of 1.3 to 1.4 given a fixed scanning angle of 135 deg. Assuming the output Stokes vectors are obtained using a commercial Stokes polarimeter (PAX5710, Thorlabs Co.) with a deviation of $\pm 10^{-3}$, the estimated resolution of the extracted R values is of the order of 10^{-4} RIU. Note that the results presented in Fig. 3(a) show that the sensitivity of the extraction results is the same given a scanning angle of 45 deg as that for a scanning

angle of 135 deg. Thus, only the data obtained for a scanning angle of 135 deg are considered in deriving Fig. 3(b).

6 Sensitivity of Circular Birefringence Measurements to Glucose Concentration

Simulations were performed to investigate the sensitivity of the extracted γ value to the change in concentration of glucose aqueous solutions. In performing the simulations, it was assumed that the refractive index increased linearly from 1.3 to 1.4 as the glucose concentration increased from 0 to 100 mg/mL.[28,29] Based on this assumption, the γ values of samples with refractive indices ranging from 1.3 to 1.4 (with a step size of 0.01) were computed using Eq. (10) for scanning angle θ in the range of 0 to 180 deg. It is noted that scanning angle θ is the angle between the original $X - Y$ coordinate system and the measured $P' - S'$ coordinate system.[27]

As shown in Fig. 4(a), the extracted optical rotation angle γ is particularly sensitive to changes in the refractive index (i.e., the glucose concentration) at polarization scanning angles of 40, 60, 120, and 135 deg. Furthermore, Fig. 4(b) shows that γ decreases with the increase of refractive index over a range of 1.3 to 1.4 given a fixed scanning angle of 135 deg. Assuming that the output Stokes vectors are again obtained using a commercial Stokes polarimeter (PAX5710, Thorlabs Co.) with a deviation of $\pm 10^{-3}$, the estimated resolution of the extracted CB values is of the order of 5×10^{-5} RIU. Note that the results presented in Fig. 4(a) show that a scanning angle of 135 deg results in the highest measurement sensitivity. Thus, only the data obtained for a scanning angle of 135 deg are considered in deriving the results presented in Fig. 4(b).

Figure 5 shows the simulation results for the sensitivity of the DOP (Δ) to changes in the refractive index (1.3 to 1.4) for glucose samples with small [Fig. 5(a)] and high [Fig. 5(b)] degrees of depolarization of $\Delta = 0.4$ and 0.85, respectively. Note that in performing the simulation, the value of Δ was calculated using Eq. (19). As shown, the extracted values of Δ are insensitive to the refractive index over the full range of the polarization scanning angle for both samples. This finding is reasonable since, although Δ is a function of both R and γ, when the refractive index increases, R increases but γ decreases (or R decreases but γ increases, depending on the scanning angle). As a result, the value of Δ remains approximately unchanged. The thickness of the isotropic/anisotropic layers of the prism coupler affects
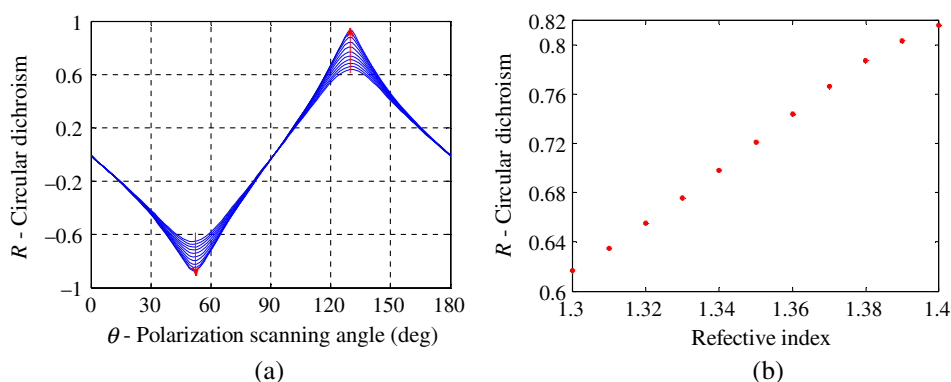

Fig. 3 (a) Variation of extracted R value with polarization scanning angle for chlorophyllin samples with refractive indices ranging from 1.3 to 1.4 (step size of 0.01). Note that the arrows show the direction of increasing refractive index. (b) Variation of extracted R value with refractive index given scanning angle of $\theta = 135$ deg. Estimated resolution of CD measurement is equal to 10^{-4} RIU.
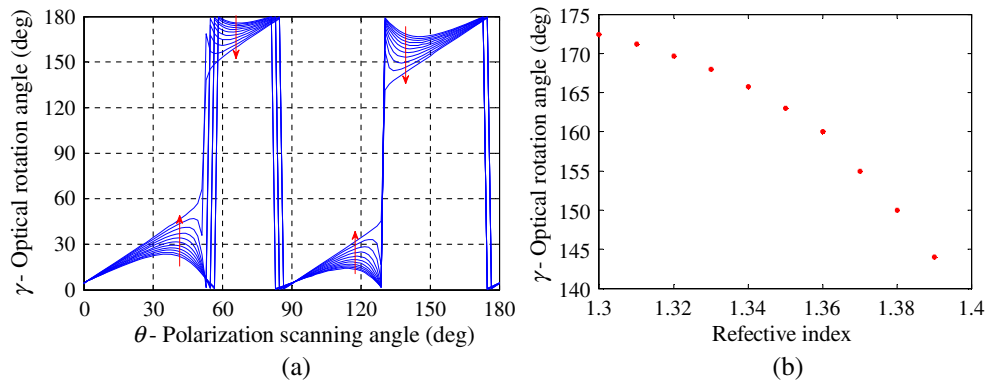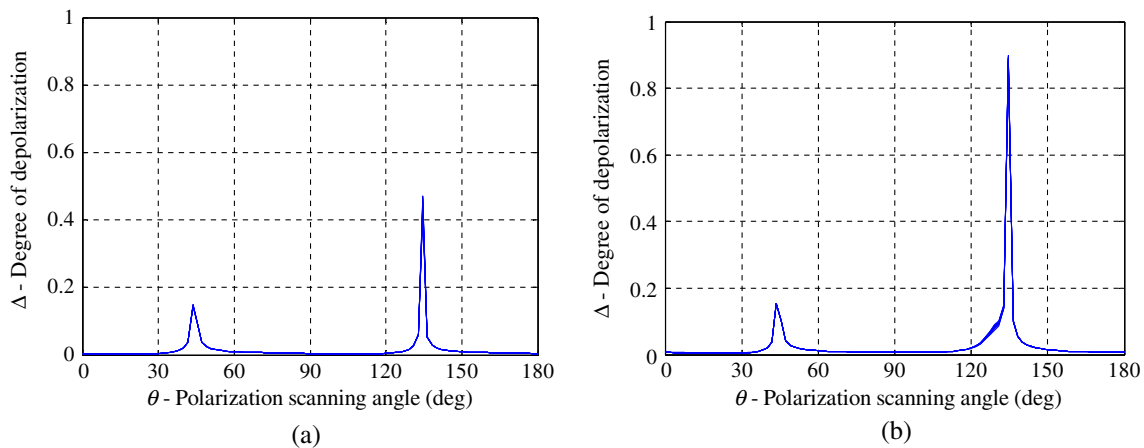
Fig. 4 (a) Variation of extracted γ value with polarization scanning angle for glucose samples with refractive indices ranging from 1.3 to 1.4 (step size of 0.01). Note that the arrows show the direction of increasing refractive index. (b) Variation of extracted γ value with refractive index given scanning angle of $\theta = 135$ deg. Estimated resolution of γ measurement is equal to 10^{-5} RIU.

Fig. 5 Variation of extracted Δ value with polarization scanning angle for glucose samples with refractive indices ranging from 1.3 to 1.4 (step size of 0.01): (a) small degree of depolarization and (b) high degree of depolarization.
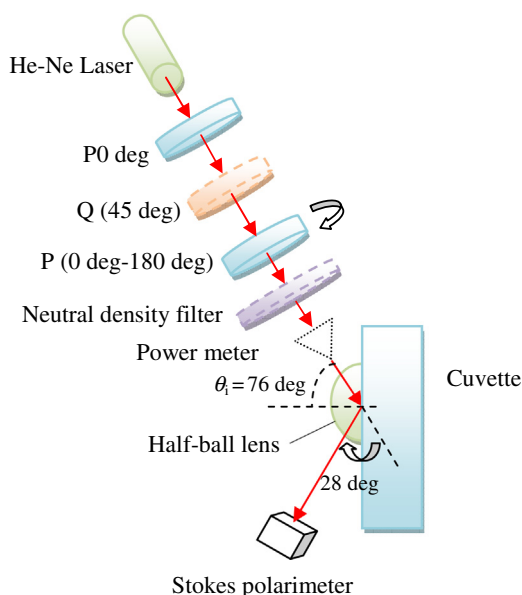

Fig. 6 Schematic illustration of experimental setup.

both the working range and the sensitivity of the sensor. Thus, the measurement sensitivity of Δ can be enhanced through an appropriate design of the prism coupler structure. In the present study, however, the prism coupler is designed only to maximize the measurement sensitivity of γ and R over the considered measurement range.

7 Experimental Setup and Results

Figure 6 presents a schematic illustration of the PSR-based scanning polarization ellipsometry system proposed in the present study. As shown, the major items of equipment include a He–Ne laser (SL 02/2, SIOS Co., central wavelength 632.8 nm), a polarizer (GTH5M, Thorlabs Co.) to produce linear polarized light, a quarter-wave plate (QWP0-633-04-4-R10, CVI Co.) to convert the linear polarized light into circular polarized light, a second polarizer (GTH5M, Thorlabs Co.) set to a scanning angle in the range of $\theta = 0$ to 180 deg, and a neutral density filter (NDC-100C-2, Oneset Co.) and power detector (8842A, OPHIR Co.) to calibrate the intensity of the input polarization light. Following the calibration process, the power detector was removed from the experimental setup, and the light emerging from the neutral density filter was reflected on the SPR sensor
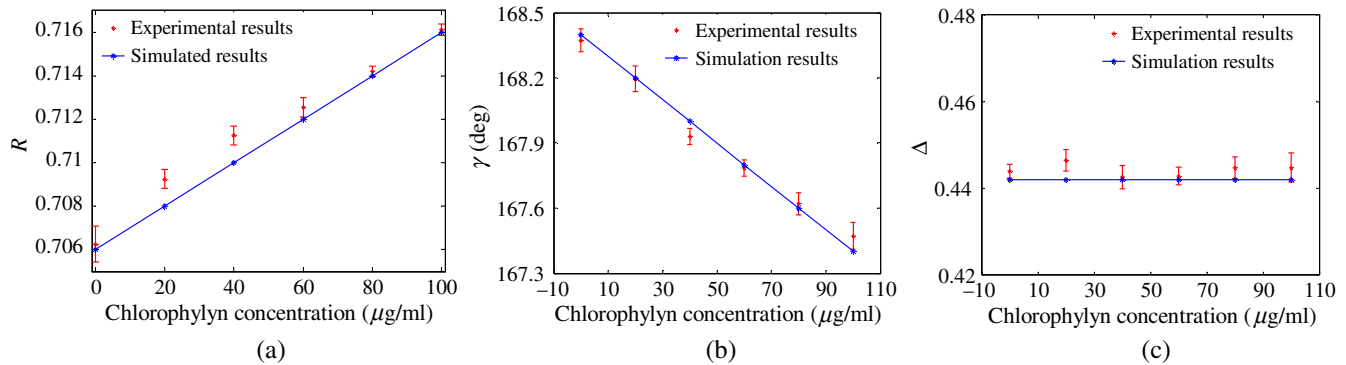
Fig. 7 Experimental and simulated results for: (a) R, (b) γ, and (c) Δ properties of CD samples with chlorophyllin concentrations ranging from 0 to 100 μg/mL. Note that the scanning angle is $\theta = 135$ deg and the incident angle is 76 deg in every case.

and detected by a commercial Stokes polarimeter (PAX5710, Thorlabs Co.). To achieve a precise alignment of the optical components in the experimental setup, a pin hole was placed in front of the polarizers and quarter-wave plate and the components were then adjusted such that the reflected laser beam passed though the pin hole in turn.

To enhance the SPR effect at the sensed interface, the Stokes polarimeter was placed on a mechanical stage (SGSP-60YAW, Sigma Koki Co.) controlled by a step motor (Mark 204-MS, Sigma Koki Co.) and rotated through an angle of 28 deg such that the incident light was incident on the prism coupler at the resonance angle of 76 deg (see Fig. 6). In performing the experiments, the linear scanning polarization lights were produced by manually rotating the second polarizer from 0 to 180 deg in steps of 15 deg using a mechanical stage (SGSP-60YAW, Sigma Koki Co.). In addition, the right-hand circular polarization light ($R-$) was produced by removing the second polarizer from the system. The samples were stored in plastic cuvettes with dimensions of $10 \times 10 \times 1$ mm. The prism coupler was attached to the cuvettes by means of industrial glue and a layer of silicon around the border edge. Prior to mounting the coupler, the cuvette was drilled with a small hole with a diameter of 6 mm such that the sample made direct contact with the half-ball lens (thereby avoiding optical interference by the cuvette material).

The CD samples were prepared using 10-mL chlorophyllin solutions (C6003, Sigma-Aldrich Co. LLC) with concentrations ranging from 0 to 100 μg/mL in 20 μg/mL increments mixed with 2 mL D-glucose solution (100 mg/mL Merck Ltd.) and 0.5-mL polystyrene microspheres (0.2 mg/mL Duke Standard™). Figure 7(a) shows the experimental and simulated R values of the chlorophyllin samples given a scanning angle of 135 deg in every case. As shown, R increases linearly with an increasing chlorophyllin concentration over the considered

concentration range. Figures 7(b) and 7(c) show the experimental and simulated values of γ and Δ, respectively, for the various samples. It is seen that γ decreases linearly with an increasing chlorophyllin concentration, while Δ remains approximately constant. The standard deviations of the measured values of R, γ, and Δ obtained on four repeated tests over the measured concentration range of chlorophyllin samples are shown in Table 1. Moreover, for all of the samples, a good qualitative agreement exists between the experimental and simulation results for all three properties. Hence, the basic validity of the proposed approach is confirmed. The slight discrepancy between the two sets of results is most likely due to alignment errors in the optical system or imperfections in the optical components themselves.

The CB samples were prepared using 10-mL glucose solution samples (100 mg/mL Merck Ltd) with concentrations ranging from 0 to 100 mg/mL in 20 mg/mL increments mixed with 2-mL chlorophyllin (C6003, Sigma-Aldrich Co. LLC) and 0.5-mL polystyrene microspheres (0.2 mg/mL Duke Standard™). Figure 8(a) shows the experimental and simulation results for the γ values of the various samples given a scanning angle of 135 deg in every case. As shown, γ decreases linearly with an increasing glucose concentration. Figures 8(b) and 8(c) show the experimental and simulation results for the R and Δ values of the various samples. It is seen that the R value increases linearly with an increasing glucose concentration, while the Δ value remains approximately constant. As for the CD samples, a good qualitative agreement exists between the experimental and simulated values in every case. The standard deviations of the measured values of γ, R, and Δ obtained on four repeated tests over the measured concentration range of glucose samples are shown in Table 2.

Overall, the results presented in Figs. 7 and 8 show that the extracted values of R and γ are linearly correlated with the

Table 1 The standard deviations of the measured values of R, γ, and Δ obtained on four repeated tests over the measured concentration range of chlorophyllin samples.

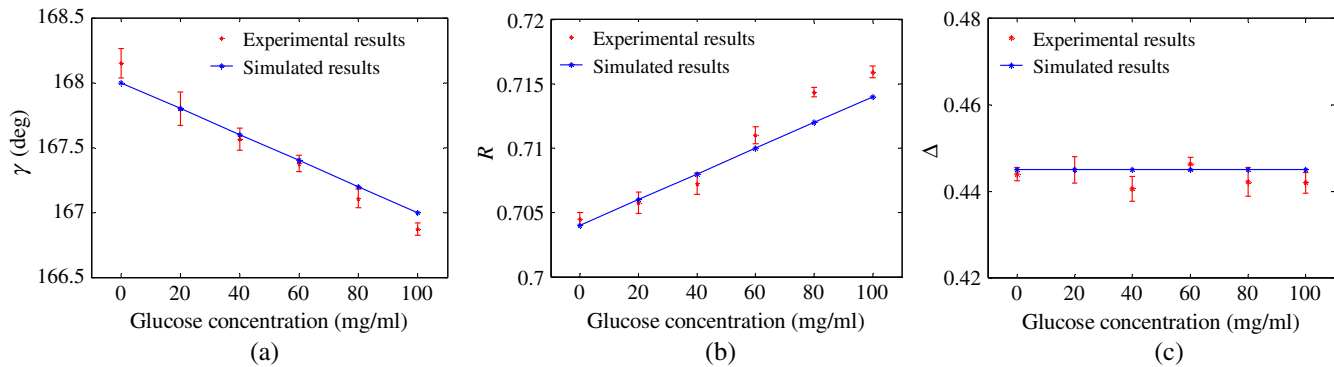| Glucose concentration		0 μg/mL	20 μg/mL	40 μg/mL	60 μg/mL	80 μg/mL	100 μg/mL
Standard deviation	R	$\pm 8.29 \times 10^{-4}$	$\pm 4.33 \times 10^{-4}$	$\pm 4.33 \times 10^{-4}$	$\pm 4.55 \times 10^{-4}$	$\pm 2.45 \times 10^{-4}$	$\pm 2.58 \times 10^{-4}$
	γ	$\pm 2.6 \times 10^{-2}$	$\pm 2.4 \times 10^{-2}$	$\pm 1.5 \times 10^{-2}$	$\pm 1.4 \times 10^{-2}$	$\pm 2.05 \times 10^{-2}$	$\pm 3.1 \times 10^{-2}$
	Δ	$\pm 1.6 \times 10^{-3}$	$\pm 2.5 \times 10^{-3}$	$\pm 2.7 \times 10^{-3}$	$\pm 2.0 \times 10^{-3}$	$\pm 2.5 \times 10^{-3}$	$\pm 3.3 \times 10^{-4}$

Fig. 8 Experimental and simulated results for: (a) γ; (b) R; and (c) Δ of CB samples with glucose concentrations ranging from 0 to 100 μg/mL. Note that the scanning angle is $\theta = 135$ deg and the incident angle is 76 deg in every case.

Table 2 The standard deviations of the measured values of γ, R, and Δ obtained on four repeated tests over the measured concentration range of glucose samples.

Glucose concentration		0 μg/mL	20 μg/mL	40 μg/mL	60 μg/mL	80 μg/mL	100 μg/mL
Standard deviation	γ	$\pm 5.0 \times 10^{-2}$	$\pm 6.1 \times 10^{-2}$	$\pm 4.2 \times 10^{-2}$	$\pm 3.2 \times 10^{-2}$	$\pm 3.5 \times 10^{-2}$	$\pm 2.4 \times 10^{-2}$
	R	$\pm 5.0 \times 10^{-4}$	$\pm 4.1 \times 10^{-4}$	$\pm 4.2 \times 10^{-4}$	$\pm 3.2 \times 10^{-4}$	$\pm 1.8 \times 10^{-4}$	$\pm 2.3 \times 10^{-4}$
	Δ	$\pm 1.6 \times 10^{-3}$	$\pm 1.5 \times 10^{-3}$	$\pm 1.4 \times 10^{-3}$	$\pm 7.5 \times 10^{-3}$	$\pm 1.6 \times 10^{-3}$	$\pm 1.2 \times 10^{-3}$

chlorophyllin and glucose concentration over the considered range. As a result, the feasibility of the proposed method for extracting the optical properties of turbid media is confirmed. In addition, the results show that the extracted Δ value is insensitive to changes in the chlorophyllin and glucose concentration over the range of 0 to 100 μg/mL and 0 to 100 mg/mL.

8 Conclusions and Suggestions

This study presents a CB/CD/DOP measurement technique based on an SPR prism coupler and Stokes–Mueller matrix polarimetry. The validity of the proposed method is demonstrated both numerically and experimentally. The simulation results show that the proposed method enables the CB and CD properties to be measured with resolutions of 10^{-5} and 10^{-4} RIU, respectively, for refractive indices in the range of 1.3 to 1.4. The simulation results also show that the measured DOP is insensitive to changes in the refractive index of the sample over the range of 1.3 to 1.4. However, in practice, the sensitivity of the Δ measurements can be enhanced through an appropriate design of the prism coupler structure. The experimental results show that the measured CB and CD values are linearly related to the chlorophyllin and glucose concentrations, respectively, over the measured range. Furthermore, the average deviations of the CD, CB, and DOP measurements over four repeated tests are approximately $\pm 1.59 \times 10^{-4}$, $\pm 4.1 \times 10^{-2}$, and $\pm 2.01 \times 10^{-3}$, respectively. Thus, the feasibility of the SPR-enhanced Stokes–Mueller matrix polarimetry technique proposed in this study for practical CB/CD/DOP sensing applications is confirmed.

Disclosures

No conflicts of interest, financial or otherwise, are declared by the authors.

References

1. A. Bhandari et al., "Stokes scattering matrix for human skin," *Appl. Opt.* **51**(31), 7487–7497 (2012).
2. S. Firdous and M. Ikram, "Stokes polarimetry for the characterization of biomaterial using liquid crystal variable retarders," *Proc. SPIE* **6632**, 66320F (2012).
3. K. Hassani and K. Abbaszadeh, "Thin film characterization with a simple Stokes ellipsometer," *Eur. J. Phys.* **36**(2), 025017 (2015).
4. N. Gosh et al., "Mueller matrix decomposition for polarized light assessment of biological tissue," *J. Biophotonics* **2**(3), 145–156 (2009).
5. S. A. Hall et al., "Combined stokes vector and Mueller matrix polarimetry for materials characterization," *Anal. Chem.* **85**(15), 7613–7619 (2013).
6. C. W. Sun et al., "Characterization of tooth structure and the dentin enamel zone based on the Stokes-Mueller calculation," *J. Biomed. Opt.* **17**(11), 116026 (2012).
7. S. Y. Lu and R. A. Chipman, "Interpretation of Mueller matrices based on polar decomposition," *J. Opt. Soc. Am. A* **13**(5), 1106–1113 (1996).
8. S. Kumar et al., "Comparative study of differential matrix and extended polar decomposition formalism for polarimetric characterization of complex tissue-like turbid media," *J. Biomed. Opt.* **17**(10), 105006 (2012).
9. N. Ghosh and I. A. Vitkin, "Tissue polarimetry: concepts, challenges, application and outlook," *J. Biomed. Opt.* **16**(11), 110801 (2011).
10. T. H. H. Pham and Y. L. Lo, "Extraction of effective parameters of anisotropic optical materials using a decoupled analytical method," *J. Biomed. Opt.* **17**(2), 025006 (2012).

11. T. H. H. Pham and Y. L. Lo, "Extraction of effective parameters of turbid media utilizing the Mueller matrix approach: study of glucose sensing," *J. Biomed. Opt.* **17**(9), 0970021 (2012).

12. N. O. Quijano et al., "Experimental validation of Mueller matrix differential decomposition," *Opt. Express* **20**(2), 1151–1163 (2012).

13. C. C. Liao and Y. L. Lo, "Extraction of anisotropic parameters of turbid media using hybrid model comprising differential and decomposition based Mueller matrices," *Opt. Express* **21**(14), 16831–16853 (2013).

14. L. Wu et al., "Highly sensitive grapheme biosensors based on surface plasmon resonance," *Opt. Exp.* **18**(14), 14395–14400 (2010).

15. Q. Fernandez et al., "Circular dichroism of chiral nematic films of cellulose nanocrystals loaded with plasmonic nanoparticles," *ACS Nano* **9**(10), 10377–10385 (2015).

16. Q. H. Phan, P. M. Yang, and Y. L. Lo, "Surface plasmon resonance prism coupler for gas sensing based on Stokes polarimetry," *Sens. Actuators B* **216**, 247–254 (2015).

17. N. Ghosh and I. A. Vitkin, "Surface plasmon resonance sensors based on diffraction gratings and prism couplers: sensitivity comparison," *Sens. Actuators B* **54**, 16–24 (1999).

18. H. Arwin, M. Poksinski, and K. Johansen, "Total internal reflection ellipsometry: principles and applications," *Appl. Opt.* **43**(15), 3028–3036 (2004).

19. N. C. H. Le et al., "Ultrathin and smooth poly (methyl methacrylate) (PMMA) films for label free biomolecule detection with total internal reflection ellipsometry (TIRE)," *Biosens. Bioelectron.* **36**(1), 250–256 (2012).

20. J. G. Olender et al., "A total internal reflectance ellipsometry and atomic force microscopy study of interactions between proteus mirabilis lipopolysaccharides and antibodies," *Eur. Biophys. J.* **44**(5), 301–307 (2015).

21. Z. Balevicius et al., "*In situ* study of ligand receptor interaction by total internal reflection ellipsometry," *Thin Film Solid* **571**, 744–748 (2014).

22. Z. Balevicius et al., "Study of optical anisotropy in thin molecular layers by total internal reflection ellipsometry," *Sens. Actuators B* **181**, 119–124 (2013).

23. Q. H. Phan, Y. L. Lo, and C. L. Huang, "Surface plasmon resonance prism coupler for enhanced circular dichroism sensing," *Opt. Express* **24**(12), 12812–12824 (2016).

24. C. Houssier and K. Sauer, "Circular dichroism and magnetic circular dichroism of the chlorophyll and protochlorophyll pigments," *J. Am. Chem. Soc.* **92**(4), 779–791 (1970).

25. R. Syafinar et al., "Chlorophyll pigments as nature based dye for dye-sensitized solar cell (DSSC)," *Energy Procedia* **79**, 896–902 (2015).

26. C. Y. Tan and Y. X. Huang, "Dependence of refractive index on concentration and temperature in electrolyte solution, polar solution, nonpolar solution and protein solution," *J. Chem. Eng. Data* **60**(10), 2827–2833 (2015).

27. Y. L. Lo, Y. F. Chung, and H. H. Lin, "Polarization scanning ellipsometry method for measuring effective ellipsometry parameters of isotropic and anisotropic thin films," *J. Lightwave Technol.* **31**(14), 2361–2369 (2013).

28. Y. L. Yeh, "Real-time measurement of glucose concentration and average refractive index using a laser interferometer," *Opt. Laser. Eng.* **46**(9), 666–670 (2008).

29. W. M. B. M. Yunus and A. B. A. Rahman, "Refractive index of solutions at high concentrations," *Appl. Opt.* **27**(16), 3341–3343 (1988).

Quoc-Hung Phan received his BS degree in mechanical engineering from Ho Chi Minh City University of Technology, Vietnam in 2004 and his MS degree in Department of Mechanical Engineering at Southern Taiwan University, Tainan, Taiwan, China. In 2016, he received his doctor's degree in the Department of Mechanical Engineering, National Cheng Kung University. His research interests include sub-wavelength sensors, polarimetry, and its application for biosensing.

Yu-Lung Lo received his BS degree from National Cheng Kung University, Tainan, Taiwan, China, in 1985, and his MS degree and PhD in mechanical engineering from the Smart Materials and Structures Research Center, University of Maryland, United States, in 1992 and 1995, respectively. His research interests include experimental mechanics, fiber-optic sensors, optical techniques in precision measurements, biophotonics, and additive manufacturing.